Surfactant-Free Palladium Nanoparticles Encapsulated in ZIF-8 Hollow Nanospheres for Size-Selective Catalysis in Liquid-Phase Solution

Xiaoshi Wang,[a, b] Mingyu Li,[c] Changyan Cao,*[a, b] Chang Liu,[a, b] Jian Liu,[a, b] Yanan Zhu,[a, b] Sidi Zhang,[a, b] and Weiguo Song*[a, b]

Encapsulation of surfactant-free Pd nanoparticles (NPs) in the metal–organic framework material ZIF-8 hollow nanospheres was achieved. Pd@ZIF-8 hollow nanospheres showed excellent size-selective catalytic properties in the liquid-phase hydrogenation of olefins. As a result of the uniform pore size of the ZIF-8 shell (apertures of 3.4 Å), the catalyst showed high activity for the hydrogenation of 1-hexene (1.9×8.2 Å) but very low activity for larger molecules such as cis-cyclooctene (5.3×5.5 Å), trans-stilbene (4.2×11.3 Å), and triphenylethylene (9.1×9.2 Å). Other surfactant-free noble-metal nanoparticles could also be employed to produce NPs@MOFs for catalysis.

Metal–organic frameworks (MOFs) have several unique properties such as uniform and tunable pore sizes, diverse structural topologies, and tunable functionalities.[1–5] These features endow MOFs with excellent abilities in a wide range of applications, including gas storage/separation, guest-dependent luminescence, catalysis, and so on.[2,6–11] Furthermore, combining the functions of MOFs with metal cores to create multifunctional core@shell nanocomposites has been extensively investigated.[12–16] Unlike other porous materials, MOFs can be used as an ideal shell material for confined catalysis and size-selective catalysis, which is of great significance for both fundamental research and industrial applications.[5,17–21]

Two common approaches have been reported to fabricate nanoparticles encapsulated in MOFs.[15,22] The first "ship-in-a-bottle" approach involves the introduction of metal precursors into the pores of the matrix of a presynthesized MOF and subsequent reduction or decomposition. The framework structure of the MOF may be damaged and some nanoparticles would then be found on the external surface.[12,23,24] The second approach is the "ship-around-a-bottle" method, which involves the assembly of MOF precursors around presynthesized nanoparticles. The size, shape, and composition of the nanoparticles can be fully encapsulated in the MOF. However, nanoparticles used in this method are usually stabilized with capping agents, which are difficult to remove and often lower the catalytic activity.[25–28]

Herein, we report a well-designed route to prepare surfactant-free Pd nanoparticles encapsulated in ZIF-8 hollow nanospheres (Scheme 1). First, Pd nanoparticles are loaded on car-
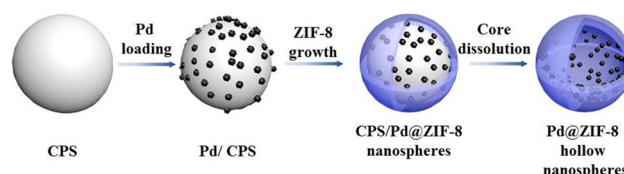
Scheme 1. Illustration of the procedure for the synthesis of Pd@ZIF-8 hollow nanospheres.

boxylate-terminated polystyrene (CPS) spheres through an in situ reduction method with Sn[II] ions.[29] During this step, the high affinity between the Sn[II] ions and the carboxyl groups ensures that the Pd nanoparticles are deposited uniformly on the surface of the CPSs. Second, by exploiting the coordination ability of the carboxyl groups with Zn ions and 2-methylimidazole, ZIF-8 are generated on the surface of CPS, and CPS/Pd@ZIF-8 core@shell composite nanospheres are obtained.[30] Finally, the CPS cores are removed by DMF to produce Pd@ZIF-8 hollow nanospheres. Through this route, all the Pd nanoparticles are encapsulated in the ZIF-8 hollow nanospheres, which can be used as an ideal nanoreactor for size-selective catalysis in liquid-phase solution.

The products obtained in each step were verified by transmission electron microscopy (TEM). Relative to the surfaces of the pure polystyrene (PS) spheres, the surfaces of the CPS spheres are more rough (Figure 1a). Figure 1b shows that Pd nanoparticles are loaded successfully on the surface of CPS. Then, a ZIF-8 layer with a thickness of approximately 40 nm is coated on the surface of Pd/CPS (Figure 1c). After etching CPS, Pd nanoparticles encapsulated in ZIF-8 hollow nanospheres are obtained (Figure 1d). It can be seen that the ZIF-8 shells remain intact during etching. The high-magnification TEM

[a] X. Wang, Dr. C. Cao, C. Liu, J. Liu, Y. Zhu, S. Zhang, Prof. Dr. W. Song
Beijing National Laboratory for Molecular Sciences
Laboratory of Molecular Nanostructures and Nanotechnology
Institution Institute of Chemistry
Chinese Academy of Sciences
Beijing 100190 (China)
E-mail: cycao@iccas.ac.cn
wsong@iccas.ac.cn

[b] X. Wang, Dr. C. Cao, C. Liu, J. Liu, Y. Zhu, S. Zhang, Prof. Dr. W. Song
University of Chinese Academy of Sciences
Beijing 100049, (P.R. China)

[c] M. Li
The Masters School
49 Clinton Ave, Dobbs ferry, New York 10522, (USA)

Supporting Information and the ORCID identification number(s) for the author(s) of this article can be found under http://dx.doi.org/10.1002/cctc.201600846.
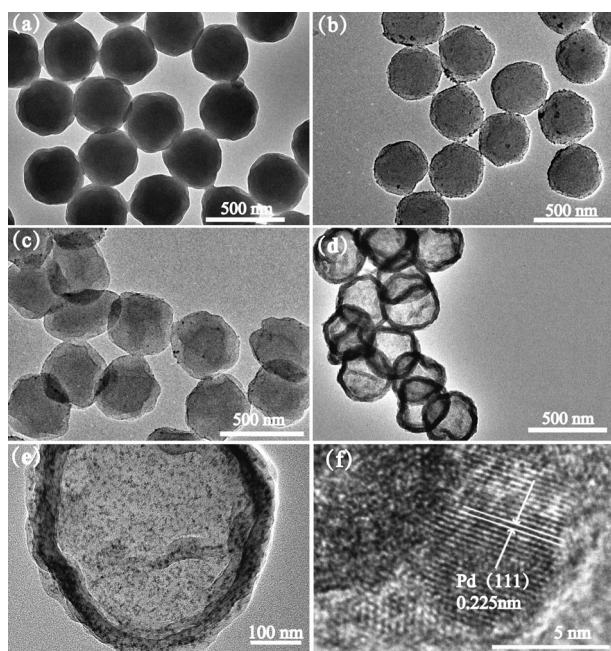
Figure 1. TEM images of a) CPS, b) Pd/CPS, c) Pd/CPS@ZIF-8, and d,e) Pd@ZIF-8 hollow nanospheres; f) HRTEM image of Pd@ZIF-8 hollow nanospheres.

image indicates that Pd nanoparticles approximately 5 nm in diameter are dispersed uniformly inside the ZIF-8 shell, and no Pd nanoparticles are observed on the external surface (Figure 1 e). The HRTEM image (Figure 1 f) shows clear lattice fringes of 0.225 nm, which correspond to the (111) planes of Pd.

Energy-dispersive spectroscopy (EDS) mapping results further reveal that Pd nanoparticles are well dispersed inside the ZIF-8 hollow nanospheres (Figure 2). X-ray photoelectron spectroscopy (XPS) is an ideal technology to detect the location of
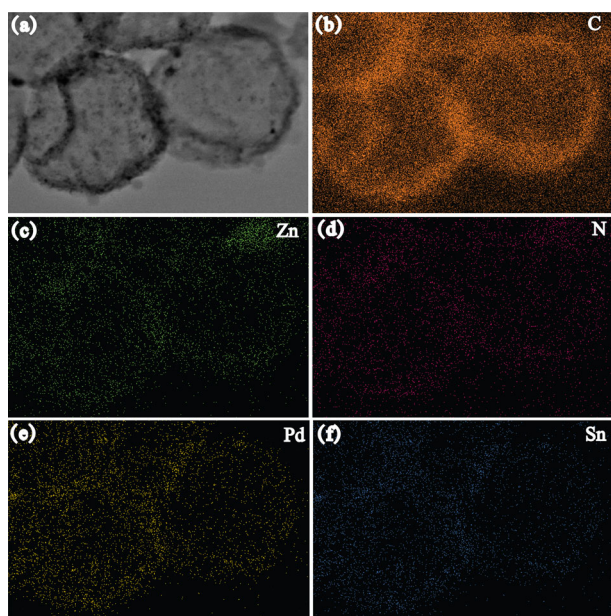
Figure 2. EDS elemental mapping of Pd@ZIF-8 hollow nanospheres.

Pd nanoparticles owing to the penetration limit of the photoelectron beam ($\approx$10 nm thickness). As shown in Figure S2 (Supporting Information), nearly no signals of Pd can be detected for Pd@ZIF-8 hollow nanospheres by XPS. For comparison, clear peaks of Pd 3d are observed for Pd nanoparticles deposited on the external surface of ZIF-8. All of the above results clarify that the Pd nanoparticles indeed resided inside the ZIF-8 shells.

The X-ray diffraction (XRD) patterns confirm that the coating layer is ZIF-8 and that the crystalline structure is retained after etching CPS for the final Pd@ZIF-8 hollow nanospheres (Figure 3 a). No clear peaks of Pd can be seen, which suggests a small size of the Pd nanoparticles and a low content of Pd in Pd@ZIF-8 hollow nanospheres. The inductively coupled plasma atomic emission spectroscopy (ICP-AES) results show that the Pd content is approximately 0.83 wt% in Pd@ZIF-8 hollow nanospheres.
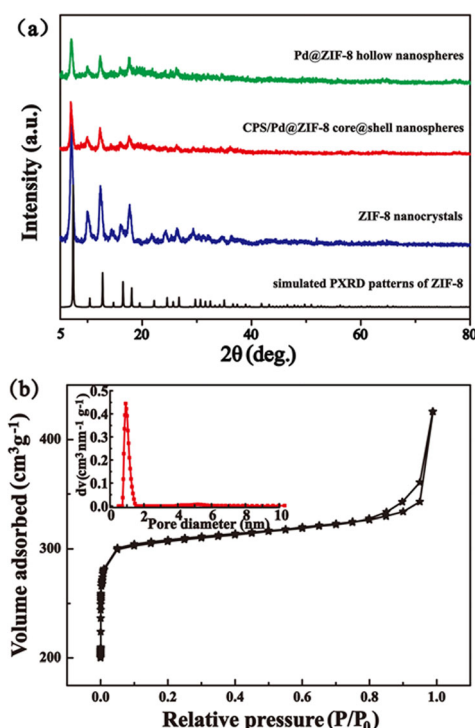
Figure 3. a) XRD pattern and b) N_2 adsorption–desorption isotherms of Pd@ZIF-8 hollow nanospheres. The inset shows the micropore size distribution curve.

The N_2 adsorption–desorption isotherm of Pd@ZIF-8 hollow nanospheres is shown in Figure 3 b. It displayed a typical type I sorption isotherm, which indicates a microporous structure of the ZIF-8 shells. A hysteresis loop at a high relative pressure of approximately $P/P_0 = 0.8$–1.0 is more likely attributed to mesopores formed by packing of the nanoparticles.[31] The Brunauer–Emmett–Teller (BET) surface area of Pd@ZIF-8 hollow nanospheres was calculated to be 934 $m^2 g^{-1}$. The nonlocal density functional theory (NLDFT) pore-size distribution (inset in Figure 3 b) suggests a central pore size of 1.0 nm for

↖↖ **These are not the final page numbers!**

Pd@ZIF-8 hollow nanospheres, which is in agreement with the pore size of ZIF-8.[32]

Considering that the particular structure of Pd@ZIF-8 hollow nanospheres, in which the Pd nanoparticles totally reside inside and ZIF-8 shell, has molecular sieving capabilities, it can be used as an ideal nanoreactor to investigate catalytic activity and size selectivity in liquid-phase solution. We chose the hydrogenation of olefins as a model reaction to probe the catalytic performance. For comparison, the hydrogenation was also performed with commercially available Pd on carbon (Pd/C), Pd nanoparticles immobilized on the outer surfaces of ZIF-8 (denoted Pd/ZIF-8), and Pd/CPS@ZIF-8.
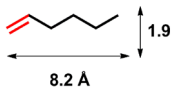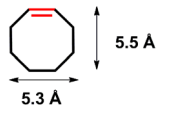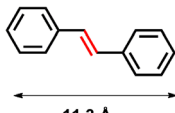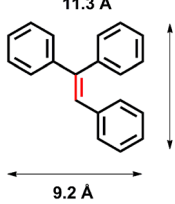
First, the kinetic curves for the hydrogenation of 1-hexene over the above four catalysts were examined, and the turnover frequencies (TOFs) are summarized in Figure S2. Pd/C and Pd/ZIF-8 showed much higher activity than Pd/CPS@ZIF-8 and Pd@ZIF-8 hollow nanospheres, which can be ascribed to the diffusion barrier of the ZIF-8 shells for mass transformation of 1-hexene.

We also found a confinement effect for catalysis on Pd@ZIF-8 hollow nanospheres. The TOF of the Pd/CPS@ZIF-8 core–shell composite nanospheres was 310 h^{-1}, which is only approximately 15% of that of Pd@ZIF-8 hollow nanospheres (2150 h^{-1}). For Pd/CPS@ZIF-8, in which the polystyrene template is not removed, the reactants are confined in the micropores, which makes it difficult for them to reach the active sites. After etching the polystyrene spheres, the cavities can be used as reactors for the reactants, which are confined in the cavities for conversion. Moreover, the catalytic performance of Pd@ZIF-8 hollow nanospheres was much better than that of ZIF-8 encapsulated with polyvinylpyrrolidone-protected Pd nanoparticles, as previously reported.[33–35]

Substrates with different sizes, including 1-hexene (1.9 × 8.2 Å), cis-cyclooctene (5.3 × 5.5 Å), trans-stilbene (4.2 × 11.3 Å), and triphenylethylene (9.1 × 9.2 Å), were then employed to study the size selectivity of Pd@ZIF-8 hollow nanospheres. As shown in Table 1, 1-hexene was converted into the corresponding product with all catalysts. On the contrary, larger sized molecules (i.e., cis-cyclooctene, trans-stilbene, and triphenylethylene) were only converted on Pd/C and Pd/ZIF-8. No products were detected on Pd/CPS@ZIF-8 and Pd@ZIF-8 hollow nanospheres, even after 24 h. The sharp difference in reactivity suggests size selectivity of Pd@ZIF-8 hollow nanospheres in liquid-phase solution. ZIF-8 has large pores of 11.6 Å and small apertures of 3.4 Å, which are bigger than the size of 1-hexene (1.9 Å), and thus, mass transformation of 1-hexene in liquid solution is facile. On the contrary, the molecular widths of cis-cyclooctene, trans-stilbene, and triphenylethylene exceed the size of the apertures in ZIF-8. Thus, they cannot diffuse through the shell to reach the encapsulated Pd nanoparticles, and consequently, no conversion is observed.

Finally, the catalytic stability of Pd@ZIF-8 hollow nanospheres was investigated. As shown in Figure S3, there was no

Table 1. Size-selective hydrogenation of olefins of different sizes.[a]

Olefin		Conversion for different catalysts[b] [%]		
	Pd/C	Pd/ZIF-8	CPS/Pd@ZIF-8 nanospheres	Pd@ZIF-8 hollow nanospheres
1.9 Å, 8.2 Å	100	100	100	100
5.5 Å, 5.3 Å	100	100	0	0
4.2 Å, 11.3 Å	100	100	0	0
9.1 Å, 9.2 Å	100	100	0	0

[a] Reaction conditions: ethanol (15 mL), 25 °C, H$_2$ (1.0 MPa), catalyst/substrate molar ratio of 1:100 (10 mmol scale), 24 h. [b] Conversion was determined by GC, and the identity was ascertained by GC–MS.

marked decrease in activity, even after 10 consecutive recycling runs for the hydrogenation of 1-hexene. The TEM image show that there was only slight aggregation of the Pd nanoparticles after reuse (Figure S4). Evidently, the yolk@shell Pd@ZIF-8 hollow nanospheres are highly stable against migration and sintering of the Pd nanoparticles and exhibit excellent activity and stability for the hydrogenation of olefins.

In summary, Pd nanoparticles encapsulated in ZIF-8 hollow nanospheres were synthesized by nucleation of ZIF-8 nanostructures around unprotected Pd nanoparticles supported on carboxylate-terminated polystyrene nanospheres. No further reduction or removal of extra capping agents was needed, and the resulting composites have a precisely controlled overall structure. The obtained Pd@ZIF-8 hollow nanospheres exhibited size-selective catalytic properties for the hydrogenation of olefins in liquid-phase solution. It is expected that other surfactant-free noble-metal nanoparticles could also be employed to fabricate NPs@MOFs with the same strategy.

Experimental Section

Preparation of carboxylate-terminated polystyrene nanospheres

Polystyrene nanospheres were prepared according to a method reported elsewhere. In a typical synthesis, a mixture of styrene (21 mL), methyl methacrylate (1.1 mL), acrylic acid (0.92 mL), and NH$_4$HCO$_3$ (0.49 g) was added to deionized water (100 mL) with mechanical stirring. Upon increasing the temperature to 70 °C, ammonium persulfate (0.53 g) was added, and the mixture was allowed to react for 12 h at 80 °C. The resulting product was separated by

These are not the final page numbers! ↗↗

centrifugation, then washed with deionized water, and freeze-dried, which led to the polystyrene nanospheres.

Preparation of Pd/polystyrene nanospheres

In a typical synthesis, carboxylate-terminated polystyrene nanospheres (100 mg) were dispersed in distilled water (50 mL), and the mixture was stirred for 10 min; then, 0.02 M HCl (20 mL) containing $SnCl_2$ (0.1 g) was added. The suspension was stirred for 10 min and was then centrifuged. After washing with distilled water ($5\times$), the precipitate was dispersed in distilled water (50 mL). Then, 0.0564 M $PdCl_2$ (100 µL) was added to the suspension. After 10 min, 0.15 M sodium formate (10 mL) was added, and the mixture was stirred for 5 h. Finally, after centrifugation and washing with distilled water ($5\times$), the precipitate was dried at 60 °C for 12 h.

Preparation of Pd/polystyrene@ZIF-8 nanospheres and Pd@ZIF-8 hollow nanospheres

First, Pd/polystyrene NP nanospheres (100 mg) were added into an aqueous solution of 2-methylimidazole (10 mL, 3.5 mol). After ultrasonic treatment for 15 min, an aqueous $Zn(NO_3)_2$ solution (1.0 mL, 0.50 mol) was introduced dropwise to the mixture, which was stirred at 25 °C for 12 h. The powder was collected by filtration, washed with water and ethanol, and vacuum dried at 80 °C for 12 h. After that, the obtained Pd/polystyrene nanospheres were immersed into DMF (100 mL), and the mixture was stirred at 25 °C for 12 h to remove the PS template, which resulted in the final Pd NPs@ZIF-8 hollow spheres.

Synthesis of ZIF-8 nanocrystal

$Zn(NO_3)_2$ (0.50 mol) and 2-methylimidazole (3.5 mol) were mixed in water at 25 °C with magnetic stirring. After stirring for 12 h, the obtained solid sample was collected and washed with deionized water and ethanol. Finally, the product was dried at 80 °C under vacuum for 6.0 h.

Synthesis of Pd/ZIF-8

Pd nanoparticles on ZIF-8 were prepared by the precursor deposition method. Typically, as-synthesized ZIF-8 (100 mg) was mixed with aqueous H_2PdCl_4 (0.5 mL) with constant stirring. The resulting composite was continuously stirred for 2 h and was then dried in air at room temperature. The synthesized samples was further dried at 150 °C overnight, which was followed by treatment in a stream of H_2/N_2 (50 mL min^{-1}/50 mL min^{-1}) at 200 °C for 5 h to yield Pd/ZIF-8.

Size-selective hydrogenation experiments

Size-selective catalysis was performed in a stainless-steel reactor equipped with a stirrer bar. Typically, the catalyst/substrate molar ratio was controlled at 1:100 (10 mmol scale) and ethanol (15 mL) was loaded into the reactor. The reactor was sealed and purged with high-purity H_2 ($3\times$) with stirring to replace the air. Then, the reactor was sealed and the H_2 pressure was adjusted to 1 MPa. The reaction was performed at room temperature and lasted for a certain time. The resulting hydrogenation products were extracted and analyzed by using a GC-2010 Plus. For the recycling test, the catalyst was recovered from the reaction solution by centrifugation without further operation and was used in the next run.

Characterization

The transmission electron microscopy (TEM) images were obtained with a JEOL 2100F electron microscope running at 100 kV. Energy-dispersive X-ray spectroscopy (EDS) analysis was performed with a TEM (JEOL 2100F) equipped with an energy-dispersive X-ray analyzer (Oxford INCA). Powder X-ray diffraction (PXRD) patterns were taken with a Rigaku model D/MAX-2500V system (CuK$_\alpha$ radiation). X-ray photoelectron spectroscopy (XPS) data were obtained with an ESCALab220i-XL electron spectrometer from VG Scientific by using 300 W AlK$_\alpha$ radiation. The nitrogen adsorption–desorption isotherms were obtained with a Quantachrome Autosorb AS-1 at 77 K. The Pd content in the material was characterized by ICP-AES (Shimadzu ICPE-9000). The conversions of reagent were measured by using GC (Shimadzu GC-2010 Plus) equipped with a flame ionization detector (FID) and a Rtx-5 capillary column (0.25 mm in diameter, 30 m in length). The identity was ascertained by GC–MS (Shimadzu GCMS-QP2010S).

[1] M. Eddaoudi, J. Kim, N. Rosi, D. Vodak, J. Wachter, M. O'Keeffe, O. M. Yaghi, *Science* **2002**, *295*, 469–472.

[2] S. Kitagawa, R. Kitaura, S. Noro, *Angew. Chem. Int. Ed.* **2004**, *43*, 2334–2375; *Angew. Chem.* **2004**, *116*, 2388–2430.

[3] S. Kitagawa, K. Uemura, *Chem. Soc. Rev.* **2005**, *34*, 109–119.

[4] N. L. Rosi, J. Eckert, M. Eddaoudi, D. T. Vodak, J. Kim, M. O'Keeffe, O. M. Yaghi, *Science* **2003**, *300*, 1127–1129.

[5] B. Smit, T. L. M. Maesen, *Nature* **2008**, *451*, 671–678.

[6] C. M. McGuirk, M. J. Katz, C. L. Stern, A. A. Sarjeant, J. T. Hupp, O. K. Farha, C. A. Mirkin, *J. Am. Chem. Soc.* **2015**, *137*, 919–925.

[7] O. M. Yaghi, G. M. Li, H. L. Li, *Nature* **1995**, *378*, 703–706.

[8] R. Banerjee, A. Phan, B. Wang, C. Knobler, H. Furukawa, M. O'Keeffe, O. M. Yaghi, *Science* **2008**, *319*, 939–943.

[9] A. Corma, H. Garcia, F. X. L. I. Llabres i Xamena, *Chem. Rev.* **2010**, *110*, 4606–4655.

[10] X. Yin, Y. Song, Y. Wang, L. Zhang, Q. Li, *Sci. China Chem.* **2014**, *57*, 135–140.

[11] S. Zhang, X. Liu, B. Liu, Z. Xia, W. Wang, Q. Yang, H. Ke, Q. Wei, G. Xie, S. Chen, S. Gao, *Sci. China Chem.* **2015**, *58*, 1032–1038.

[12] A. Aijaz, Q.-L. Zhu, N. Tsumori, T. Akita, Q. Xu, *Chem. Commun.* **2015**, *51*, 2577–2580.

[13] H.-L. Jiang, T. Akita, T. Ishida, M. Haruta, Q. Xu, *J. Am. Chem. Soc.* **2011**, *133*, 1304–1306.

[14] W. Xia, R. Zou, L. An, D. Xia, S. Guo, *Energy Environ. Sci.* **2015**, *8*, 568–576.

[15] P. Hu, J. V. Morabito, C.-K. Tsung, *ACS Catal.* **2014**, *4*, 4409–4419.

[16] Y. Liu, P. Gao, C. Huang, Y. Li, *Sci. China Chem.* **2015**, *58*, 1553–1560.

[17] P. Wang, J. Zhao, X. Li, Y. Yang, Q. Yang, C. Li, *Chem. Commun.* **2013**, *49*, 3330–3332.

[18] Z. Chen, Z.-M. Cui, P. Li, C.-Y. Cao, Y.-L. Hong, Z.-Y. Wu, W.-G. Song, *J. Phys. Chem. C* **2012**, *116*, 14986–14991.

[19] C. Liu, J. Liu, S. Yang, C. Cao, W. Song, *ChemCatChem* **2016**, *8*, 1279–1282.

[20] Z.-A. Qiao, P. Zhang, S.-H. Chai, M. Chi, G. M. Veith, N. C. Gallego, M. Kidder, S. Dai, *J. Am. Chem. Soc.* **2014**, *136*, 11260–11263.

[21] M. Zhao, K. Deng, L. He, Y. Liu, G. Li, H. Zhao, Z. Tang, *J. Am. Chem. Soc.* **2014**, *136*, 1738–1741.

[22] X. Xu, Z. Zhang, X. Wang, *Adv. Mater.* **2015**, *27*, 5365–5371.

↖↖ These are not the final page numbers!

[23] M. Meilikhov, K. Yusenko, R. A. Fischer, *J. Am. Chem. Soc.* **2009**, *131*, 9644–9645.

[24] M. Müller, O. I. Lebedev, R. A. Fischer, *J. Mater. Chem.* **2008**, *18*, 5274–5281.

[25] G. Lu, S. Li, Z. Guo, O. K. Farha, B. G. Hauser, X. Qi, Y. Wang, X. Wang, S. Han, X. Liu, J. S. DuChene, H. Zhang, Q. Zhang, X. Chen, J. Ma, S. C. J. Loo, W. D. Wei, Y. Yang, J. T. Hupp, F. Huo, *Nat. Chem.* **2012**, *4*, 310–316.

[26] H. Mao, S. Peng, H. Yu, J. Chen, S. Zhao, F. Huo, *J. Mater. Chem. A* **2014**, *2*, 5847–5851.

[27] W. Zhang, G. Lu, C. Cui, Y. Liu, S. Li, W. Yan, C. Xing, Y. R. Chi, Y. Yang, F. Huo, *Adv. Mater.* **2014**, *26*, 4056–4060.

[28] W. Zhang, Y. Liu, G. Lu, Y. Wang, S. Li, C. Cui, J. Wu, Z. Xu, D. Tian, W. Huang, J. S. DuCheneu, W. D. Wei, H. Chen, Y. Yang, F. Huo, *Adv. Mater.* **2015**, *27*, 2923–2929.

[29] L.-S. Zhong, J.-S. Hu, Z.-M. Cui, L.-J. Wan, W.-G. Song, *Chem. Mater.* **2007**, *19*, 4557–4562.

[30] H. J. Lee, W. Cho, M. Oh, *Chem. Commun.* **2012**, *48*, 221–223.

[31] F. Zhang, Y. Wei, X. Wu, H. Jiang, W. Wang, H. Li, *J. Am. Chem. Soc.* **2014**, *136*, 13963–13966.

[32] K. S. Park, Z. Ni, A. P. Cote, J. Y. Choi, R. Huang, F. J. Uribe-Romo, H. K. Chae, M. O'Keeffe, O. M. Yaghi, *Proc. Natl. Acad. Sci. USA* **2006**, *103*, 10186–10191.

[33] W. Dong, C. Feng, L. Zhang, N. Shang, S. Gao, C. Wang, Z. Wang, *Catal. Lett.* **2016**, *146*, 117–125.

[34] C. Wang, H. Zhang, C. Feng, S. Gao, N. Shang, Z. Wang, *Catal. Commun.* **2015**, *72*, 29–32.

[35] Q. Yang, Q. Xu, S.-H. Yu, H.-L. Jiang, *Angew. Chem. Int. Ed.* **2016**, *55*, 3685–3689; *Angew. Chem.* **2016**, *128*, 3749–3753.
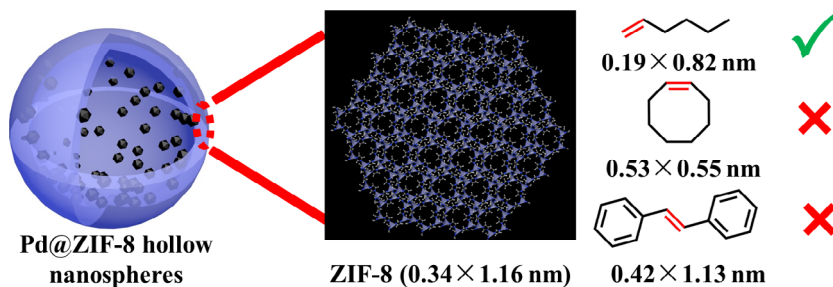
These are not the final page numbers! ↗↗

COMMUNICATIONS

X. Wang, M. Li, C. Cao,* C. Liu, J. Liu,
Y. Zhu, S. Zhang, W. Song*

■■ – ■■

Surfactant-Free Palladium
Nanoparticles Encapsulated in ZIF-8
Hollow Nanospheres for Size-Selective
Catalysis in Liquid-Phase Solution

Pd@ZIF-8 hollow nanospheres

ZIF-8 (0.34×1.16 nm)

0.19×0.82 nm ✓

0.53×0.55 nm ✗

0.42×1.13 nm ✗

Size matters: The encapsulation of surfactant-free Pd nanoparticles in ZIF-8 hollow nanospheres is achieved. Pd@ZIF-8 hollow nanospheres show excellent size-selective catalysis properties in the liquid-phase hydrogenation of olefins. As a result of the uniform pore size of the ZIF-8 shell, the catalyst shows high activity for the hydrogenation of 1-hexene but very low activity for larger molecules such as *cis*-cyclooctene and *trans*-stilbene.

↖↖ **These are not the final page numbers!**